Size-Dependent Accumulation of PEGylated Silane-Coated Magnetic Iron Oxide Nanoparticles in Murine Tumors

Esben K. U. Larsen,[†] Thomas Nielsen,[‡] Thomas Wittenborn,[‡] Henrik Birkedal,[†] Thomas Vorup-Jensen,[†] Mogens H. Jakobsen,[§] Leif Østergaard,[‡] Michael R. Horsman,[‡] Flemming Besenbacher,[†,*] Kenneth A. Howard,[†] and Jørgen Kjems[†,*]

[†]Interdisciplinary Nanoscience Center (iNANO), Departments of Molecular Biology, Physics and Astronomy, Chemistry, and Medical Microbiology & Immunology, Aarhus University, DK-8000 Aarhus C, Denmark, [‡]iNANO, Department of Experimental Clinical Oncology and Department of Neuroradiology, Danish National Research Foundations Center of Functionally Integrative Neuroscience Aarhus University Hospital, DK-8000 Aarhus C, Denmark, and [§]DTU Nanotech, Department of Micro- and Nanotechnology, DK-2800 Kongens Lyngby, Denmark

ABSTRACT Magnetic nanoparticles (MNP) can be used as contrast-enhancing agents to visualize tumors by magnetic resonance imaging (MRI). Here we describe an easy synthesis method of magnetic nanoparticles coated with polyethylene glycol (PEG) and demonstrate size-dependent accumulation in murine tumors following intravenous injection. Biocompatible iron oxide MNPs coated with PEG were prepared by replacing oleic acid with a biocompatible and commercially available silane-PEG to provide an easy and effective method for chemical coating. The colloidal stable PEGylated MNPs were magnetically separated into two distinct size subpopulations of 20 and 40 nm mean diameters with increased phagocytic uptake observed for the 40 nm size range *in vitro*. MRI detection revealed greater iron accumulation in murine tumors for 40 nm nanoparticles after intravenous injection. The enhanced MRI contrast of the larger MNPs in the tumor may be a combined result of the size-dependent extravasation and capture by macrophages in the tumor, providing important considerations for improved bioimaging approaches.

KEYWORDS: magnetic resonance imaging · cancer · magnetite nanoparticles · drug delivery · ultrasmall superparamagnetic iron oxide (USPIO) particles · polyethylene glycol

Magnetic nanoparticles (MNPs) have been synthesized and used as contrast-enhancing agents in magnetic resonance imaging (MRI) for diagnostic application in a diverse range of diseases including cardiovascular, neurological disorders, and cancer.[1−3] MNP surface coating with dextran or citrate facilitates monodispersed particles, colloidal stability, and biocompatibility that are crucial requirements for clinical application.[4,5] Furthermore, coating the particles with oleic acid can create a hydrophobic surface that reduces particle oxidation.[6] Subsequent replacement of oleic acid with alternative compounds, such as silane, allows greater flexibility with regard to surface chemistry modification and biocompatibility.[7−9] Commercially available end-labeled silane derivatives allow for the introduction of different chemical moieties such as amine groups or polyethylene glycol (PEG) onto the surface of MNPs.[10] The hydrophilic PEG molecules have been used to reduce phagocytic capture of nanoparticles by cellular components of the immune system, leading to extended circulation and subsequent accumulation in tumors as a consequence of the enhanced permeability and retention (EPR) effect due to leaky vasculature and poor lymphatic drainage in tumors.[11−15] The EPR effect occurs because the newly formed vessels in the tumor are irregular in shape, leaky with large openings, and have poor lymphatic drainage. The EPR effect can be utilized for passive targeting of nanoparticles in areas with increased angiogenesis, where there is enhanced permeability of the nanoparticles out of the blood vessels and a longer retention time in the tumor.

This approach has been utilized in the development of the commercial PEGylated liposomal Doxil as an anticancer treatment.[16] The application and characterization of PEGylated approaches for silated PEG MNP-mediated imaging of tumors is unexplored.

In this work, we describe the preparation and characterization of silane-PEG-coated MNPs using a simple synthesis method based on the use of biocompatible silane-PEG as a coating agent. The effect of size on phagocytic capture of PEGylated MNPs *in vitro* and tumor accumulation *in vivo* using MRI is determined for optimal design of diagnostic nanoparticles.

*Address correspondence to fbe@inano.dk, kjems@inano.dk.

Received for review April 2, 2009 and accepted June 22, 2009.

Published online July 2, 2009.
10.1021/nn900330m CCC: $40.75

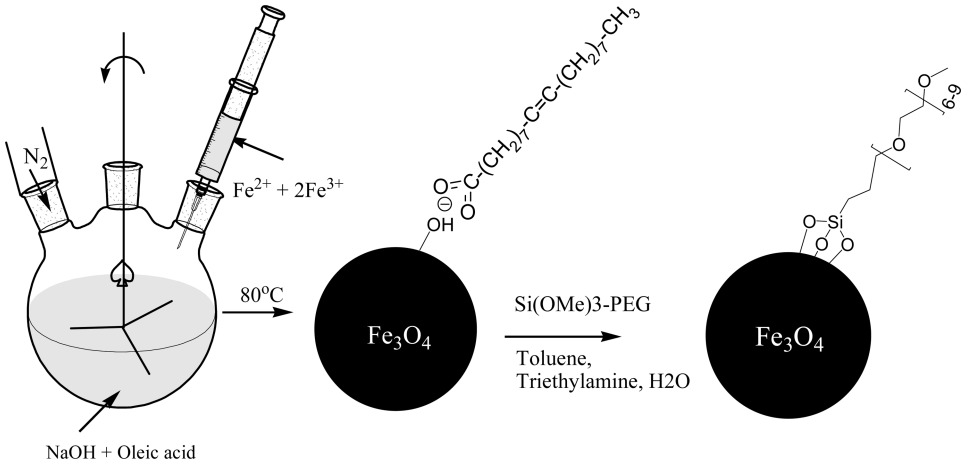

Figure 1. Preparation of PEGylated nanoparticles. Precipitation of iron ions in the presence of oleic acid yields oleic-acid-coated nanoparticles. Ligand exchange with silane-PEG replaces the oleic acid with silane, resulting in PEGylated MNPs.

RESULTS AND DISCUSSION

Iron oxide MNPs were produced and coated with 2-methoxy polyethyleneoxy propyltrimethoxysilane (silane-PEG) by a two-step method; in the first step, iron oxide MNPs were prepared by co-precipitation of Fe ions with oleic acid under basic conditions followed by a second step in toluene, where oleic acid was replaced by a silane group (Figure 1).

Fe_3O_4 nanoparticles were synthesized according to the method of Sun *et al.*[7] Replacement of oleic acid with silane-PEG was performed by a ligand exchange reaction in a toluene solvent in the presence of the base triethylamine and water. Addition of water converts the $Si(OMe)_3$ to the silanol form, enabling efficient reaction with the oxygen on the iron oxide particles and oleic acid replacement.[17] The silanol forms polymer networks up to three binding sites per Si atom to the iron oxide, resulting in a more stable coat compared to oleic acid.[8] The silane-PEG-coated nanoparticles were soluble in aqueous and organic conditions and stable to aggregation in aqueous buffer for more than 6 months at room temperature (data not shown).

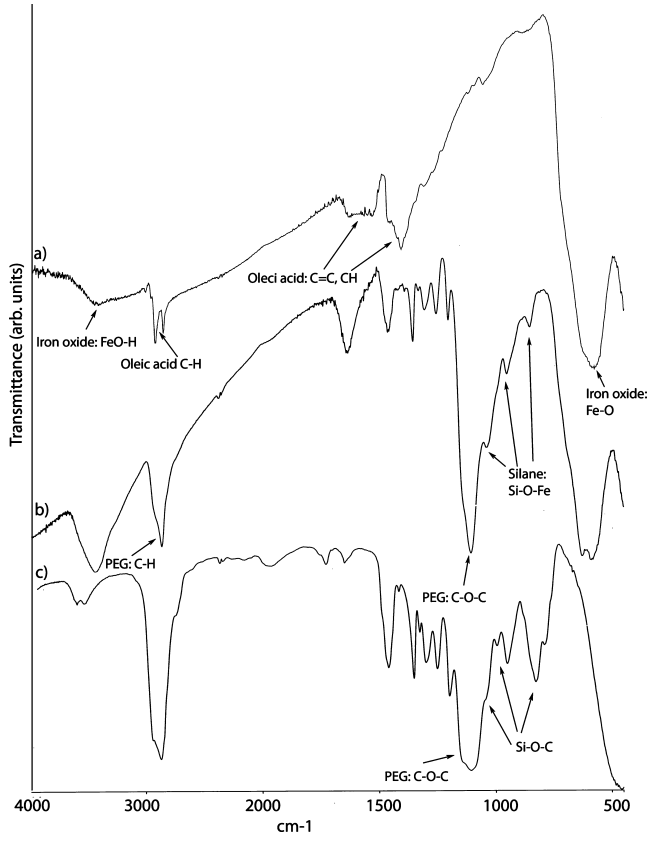

Figure 2. Infrared spectra of (a) oleic-acid-coated MNPs, (b) silane-PEG-coated MNPs, and (c) pure silane-PEG.

After purification by a toluene/pentane wash, MNPs with oleic acid and silane/PEG coatings were analyzed by IR spectroscopy (Figure 2). From the IR spectra of iron oxide particles coated with oleic acid, vibration frequencies within the crystal structure compatible with Fe−O and FeO−H bonds were detected (at 577 and 3400 cm^{-1}, respectively). The peak at 1406 cm^{-1} was attributed to C−H bending vibrations. The broad peak from 1500 to 1700 cm^{-1} represented the stretching vibration of C−C, C═C, and C═O bonds in the oleic acid carbon chain and the acid group. The oleic acid hydrocarbon chain had a distinct C−H stretching vibration at 2850−2950 cm^{-1}. Hence, all of the peaks are in accordance with previously reported spectra of oleic-acid-coated MNPs.[7]

In the IR spectra of silane-PEG-coated MNPs, the Si−O−Fe and Fe−OH peaks were detected in the frequency regimen between 500 and 1000 cm^{-1}. The peak at 1105 cm^{-1} most probably reflects C−O−C stretching vibration from the ether group. The C−H bending vibrations from the carbon chain from 1200 to 1500 cm^{-1} were difficult to assign. The peak, however, at 1344 cm^{-1} most likely derives from the C−H bending in the ether groups. Our results are in agreement with previously reported IR spectra for silane-PEG-coated MNPs.[17] The spectra are similar to the spectra of the pure silane-PEG spectra except that the pure silane-PEG does not have an absorption from iron between 500 and 600 cm^{-1}.

Transmission electron microscopy (TEM) analysis revealed a diameter of 8.0 ± 1.4 nm for the oleic-acid-coated MNP and 8.2 ± 1.7 nm for the silane/PEG-coated particles (Supporting Information Figure S1). X-ray diffraction of silane-PEG-coated MNPs showed a crystallinic Fe_3O_4 core structure with diameters between 11 and 15 nm (Table S2 and Figure S2 in Supporting Infor-

mation). The hydrodynamic radius of the MNPs measured by dynamic light scattering (DLS) showed a peak diameter of 26 nm and a polydispersity index of 0.24 for the PEGylated particles (Supporting Information Figure S3). This supports that the particles were discrete PEGylated particles without interparticle cross-linking previously observed with the silane coating process.[18]

The surface charge measured by the ζ potential measurement of the PEG-coated particles revealed a net charge between +27 mV (pH = 2) and −18 mV (pH = 10) with the isoelectric point at pH = 5 (Supporting Information Figure S4). These charges are probably derived from the ionizable hydroxyl groups on the iron oxide surface. Furthermore, the PEG layer inhibited particle aggregation over a period of evaluation of 1 month. The molecular density of the silane-PEG coat on the surface of MNPs was characterized by a thermogravimetric analysis performed over a temperature range of 20−900 °C (Supporting Information Figure S5). On the basis of the total weight loss of 30% (w/w), and assuming an average size of 8 nm, we estimated a silane-PEG surface density of 10.5 molecules per nm^2 MNP surface. The cellular cytotoxicity in HeLa cells was measured after 24 h incubation by a colorimetric MTT cell viability assay to determine the clinical feasibility of the nanoparticles (Supporting Information Figure S6). A 90−100% cell viability was observed in the cells incubated with silane-PEG-coated iron oxide at 1.6−200 μg/mL concentration, suggesting the nontoxic nature of the MNPs.[19]

Two batches of differently sized silane-PEG-coated particles were synthesized by magnetic separation using a neodymium magnet attached to a MACS column in which larger nanoparticles were retained and smaller particles contained within the effluent. DLS measurements revealed effluent-containing small MNPs with a mean diameter of ~20 nm, whereas the retained MNPs were significantly larger with a mean diameter of ~40 nm. TEM analysis revealed iron oxide cores with a mean diameter at 4.6 ± 1.4 nm for the 20 nm particles compared to 9.4 ± 1.9 nm for the larger 40 nm particles (Figure 3).

The macrophage cell line RAW 264.7 was used as a cellular model for phagocytic capture of the nanoparticles at a concentration range of 0.1−0.4 mg/mL over a 24 h incubation. After repeated cell washes, the total iron and protein contents in the cell culture were measured using ferrozin and Bradford assay, respectively (Figure 4). Compared to the 20 nm particles, the uptake of 40 nm particles exhibited an ~8-fold increase, suggesting that the phagocytic uptake is size-dependent. However, the 40 nm particles have 8 times larger volume compared to the 20 nm particles, which indicates a similar number of particle uptake. The size-dependent nature of macrophage phagocytosis has been described previously for various other types of nanoparticles with larger particles showing greater uptake.[20] Studies of macrophage uptake of iron oxide MNPs has revealed a dependence on the polyanion scavenger receptor SR-A, which can recognize negative charged particles.[21] Receptor-mediated uptake can explain the increased uptake, in weight, of the larger nanoparticles as each nanoparticle is taken up specifically.

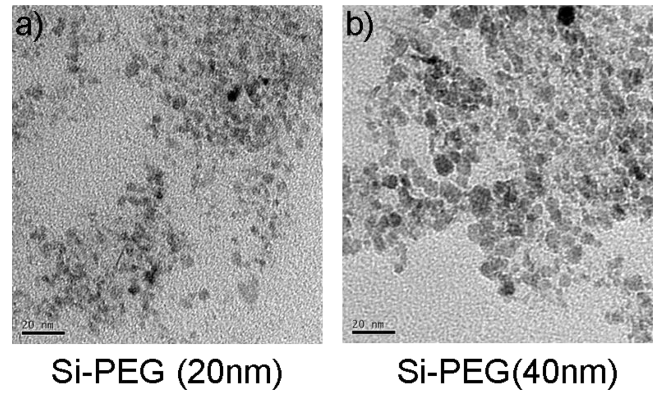

Figure 3. Size range of magnetically separated PEGylated iron oxide nanoparticle analyzed by TEM. (a) Small 20 nm silane-PEG-coated MNPs have an iron oxide core with an average size of 4.6 ± 1.4 nm. (b) Larger 40 nm silane-PEG-coated MNPs have an average iron oxide core of 9.4 ± 2.0 nm (scale bar = 20 nm).

Interestingly, the PEG coat did not inhibit cellular uptake, promoting the use of the 40 nm magnetic nanoparticles for macrophage imaging applications *in vivo*.

Mice bearing subcutaneously implanted foot tumors were examined by MRI before and after intravenous injection with either 20 or 40 nm MNPs or a non-separated mixture of MNPs (Figure 5). As a measure of accumulation, the relaxation rate R_2 was used due to the correlation with accumulation of nanoparticles.

Before injection, the R_2 value in the tumor was measured to be 20 s^{-1}. After 24 h, this increased to over 30 s^{-1} for mice injected with the nonseparated particles and the larger 40 nm particles (Figure 5a,c). In contrast, the small 20 nm particles did not result in any increased contrast within the tumor (Figure 5b).

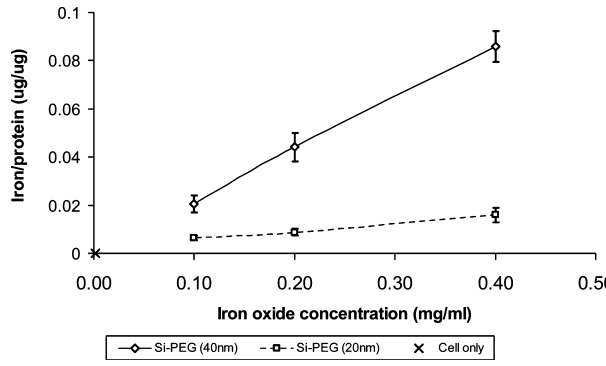

Figure 4. Uptake of different sized iron oxide nanoparticles in macrophage-like cells (RAW 264.7). Concentration-dependent uptake was observed, with approximately 8-fold lower uptake of the small (20 nm) particles compared to the larger (40 nm) particles. The mean cellular uptake and standard deviation error bars are shown. All samples were performed in triplicates.

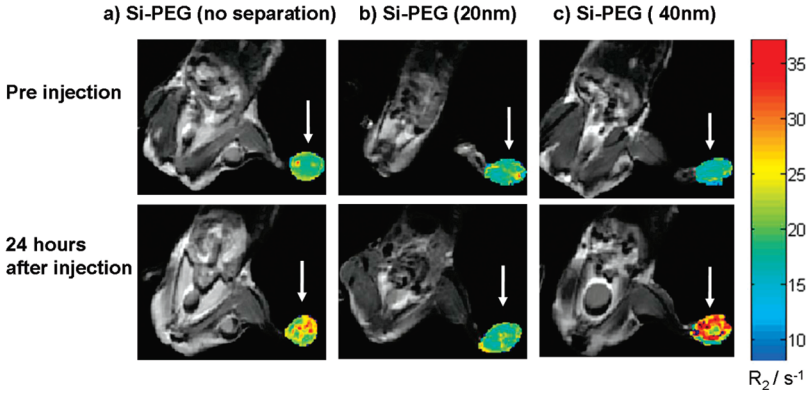

Figure 5. MRI in mice with a SCCVII tumor before and 24 h after injection of MNPs. Tumor R_2 map overlay (arrow) on a T_2-weighted MRI image. (a) MRI of the PEGylated nanoparticles without magnetic separation showed increased R_2 values in the tumor after injection of the MNPs. (b) Injection of the 20 nm MNPs did not change the R_2 value in the tumor. (c) Injection of the 40 nm MNPs gave rise to higher R_2 values in the tumor.

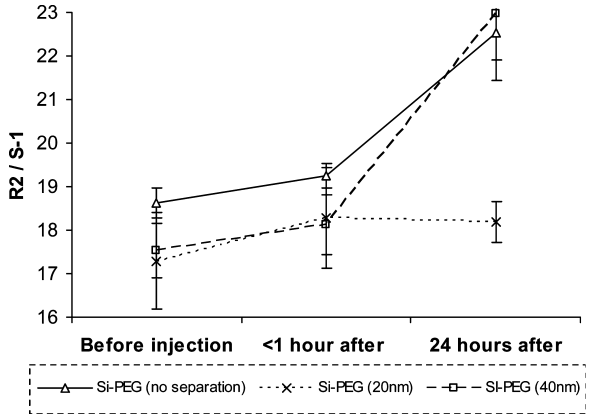

Figure 6. Quantification of average R_2 values when different sized iron oxide nanoparticles were injected into mice with a SCCVII tumor. R_2 values are averaged over a region of interest around the tumor. The nonseparated and the larger particles give a greater contrast difference. The values are averaged from two animals in each of the Si-PEG and Si-PEG (20 nm) groups and four animals in the Si-PEG (40 nm) group, with error bars showing the standard deviation.

The larger nanoparticles exhibited a significant increase in contrast in the tumor after 24 h. To quantify this difference, a region of interest (ROI) was selected around the tumor on the MRI image, and the R_2 value was measured before and after injection (Figure 6). The 40 nm PEG-coated nanoparticles resulted in a 31 ± 9% higher contrast relative to preinjection. The contrast change of the 40 nm particles is significantly larger than the 20 nm and had a contrast change of 5 ± 3%. Contrast change of the nonseparated particles was 20 ± 3% and is slightly lower compared to that of the 40 nm particles. This is probably due to the lower content of larger MNPs in this fraction.

Direct extravasation of particles out across all blood vessels has been described for nanoparticles with a crystal size below 9 nm.[22] The small 20 nm particles with a crystal size of 4.6 ± 1.4 nm could result in loss into other tissues, while the 40 nm particles with a crystal size above 9 nm are restricted to extravasate in the tumor by the EPR effect. In addition, the smaller nanoparticles may be able to re-enter the bloodstream and deplete the amount retained within the tumor.

The increased entry of the 40 nm particles into tumor tissue may also be attributed to the increased entry into macrophages. It has previously been reported that tumor-associated macrophages can capture nanoparticles at the tumor site.[23] The accumulation of the 40 nm particles in the tumor could, therefore, be a combined effect of the particle-specific extravasation and capture by macrophages in the tumor.

In summary, biocompatible iron oxide MNPs coated with commercial PEG-silane were prepared by a simple synthesis method in which oleic acid was replaced with silane-PEG to provide an easy and effective method for chemical coating or conjugation of bioactive molecules. The colloidal stable PEGylated MNPs were magnetically separated into two distinct size subpopulations that exhibited different accumulation into macrophages *in vitro* and murine tumors after intravenous injection. The enhanced MRI contrast in the tumor of the larger MNPs could be attributed to the combined effect of size-dependent extravasation and capture by macrophages in the tumor, an important consideration for improved bioimaging approaches.

METHODS

Materials. Oleic acid, *N*-hydroxysuccinimide (NHS), pentane, toluene, iron(III) chloride pentahydrate, iron(II) chloride tetrahydrate, sodium hydroxide, and triethylamine (TEA) were all purchased from Sigma-Aldrich. FerroZine iron reagent solution was from HACH; msMACH columns were from Miltenyi Biotec. Neodymium rare earth magnets were from Indigo. TEM grid and kohle lochfilme were from Plano. 2-Methoxy(polyethyleneoxy)propyltrimethoxysilane (Si-PEG, 596−725 Da) wsa from Gelest Inc.

In a typical experiment, synthesis of oleic-acid-coated iron particles was prepared by dissolving $FeCl_3$ and $FeCl_2$ (2:1) in water (20 mL). NaOH (50 mL, 1 M), acetone (25 mL), and oleic acid (0.5 mL) were heated to 83 °C in a flask (Figure 1). During rapid stirring (1200 rpm) under nitrogen flow, the iron solution was added dropwise over 5 min. Thereafter, oleic acid (2.5 mL) was added. After 10 min, the solution was precipitated with MeOH/acetone (1:1), centrifuged, and the supernatant discarded. This washing procedure was repeated three times.

Iron oxide nanoparticles coated with oleic acid were dissolved in toluene in a glass tube (2 mg/mL). Silane-PEG (200 μL, Gelest Inc.), triethylamine (1 mL), and H_2O (20 μL) were added to the solution while stirring. After 24 h, the particles were precipitated with pentane and centrifuged, and the supernatant was discarded. The particles were then redissolved in toluene and precipitated with pentane. This washing procedure was repeated three times.

Different fractions of MNPs coated with silane-PEG were prepared by running the samples through a magnetic msMACS column (Miltenyi Biotec) with a neodymium magnet attached.

To measure uptake in macrophages, the iron oxide nanoparticles were added to RAW cells and incubated for 24 h. After washing and harvesting the cells by trypsin treatment, the cells were lysed in passive lysis buffer from Promega, and the protein content in the cell lysate was measured with a Bradford assay. The iron concentration was determined with ferrozin assay after dissolving in HCl.

Cytotoxicity was determined using a tetrazolium-based viability assay.

SCCVII tumors were implanted into the right rear foot of female C3H/Hentac mice and grown to 200 mm^3. The MNPs were diluted in saline to the concentration of 1.25 mg Fe/mL and injected intravenously at the dose of 2.5 mg/kg animal body weight. MRI was performed using a 3 T MR scanner (Signa Excite HD). R_1, R_2, and R_2* spin echo inversion recovery, gradient echo, and spin echo sequence relaxometry was performed prior to and at different time points following intravenous contrast agent administration. All experiments were performed under national and European Union approved guidelines for animal welfare.

IR spectroscopy was performed using a Perkin-Elmer Paragon 1000 FTIR spectrometer. The samples were air-dried and then mixed with potassium bromide and pressed to a KBr disk. Thermal gravimetric analysis (TGA) was performed using a Netsch STA 409 thermal analyzer. The sample was heated from room temperature to 1100 °C at 10 K/min. Photon correlation scattering and ζ sizing was performed with a Zetasizer (Malvern Instruments, Malvern, UK).

Transmission electron microscopy was performed on samples air-dried onto 300 mesh copper grids and visualized using a 200 kV Philips CM20 microscope. For each MNP formulation, the mean size value was calculated ± standard deviation based on more than 50 particles. X-ray powder diffraction was measured on a Bruker D8 powder diffractometer using Cu $K\alpha_1$ radiation ($\lambda = 1.54056$ Å) with an Fe fluorescence suppressing detector.

Acknowledgment. This work was supported by grants from The Danish Council for Strategic Research/Programme Commission on Nanoscience, Biotechnology, and IT (NABIIT) and the Danish National Research Council, and from the Carlsberg Foundation.

Supporting Information Available: Additional experimental details, figures, and table. This material is available free of charge *via* the Internet at http://pubs.acs.org.

REFERENCES AND NOTES

1. Wickline, S A.; Neubauer, A. M.; Winter, P. M.; Caruthers, S. D.; Lanza, G. M. Molecular Imaging and Therapy of Atherosclerosis with Targeted Nanoparticles. *J. Magn. Reson. Imaging* **2007**, *25*, 667–680.
2. Jain, T. K.; Reddy, M. K.; Morales, M. A.; Leslie-Pelecky, D. L.; Labhasetwar, V. Biodistribution, Clearance, and Biocompatibility of Iron Oxide Magnetic Nanoparticles in Rats. *Mol. Pharmaceutics* **2008**, *5*, 316–327.
3. McCarthy, J. R.; Weissleder, R. Multifunctional Magnetic Nanoparticles for Targeted Imaging and Therapy. *Adv. Drug Delivery Rev.* **2008**, *60*, 1241–1251.
4. LaConte, L.; Nitin, N.; Bao, G. Magnetic Nanoparticle Probes. *Mater. Today* **2005**, *8*, 32–38.
5. Wang, Y.-X. J.; Hussain, S. M.; Krestin, G. P. Superparamagnetic Iron Oxide Contrast Agents: Physicochemical Characteristics and Applications in MR Imaging. *Eur. Radiol.* **2001**, *11*, 2319.
6. Maity, D.; Agrawal, D. C. Synthesis of Iron Oxide Nanoparticles under Oxidizing Environment and Their Stabilization in Aqueous and Non-aqueous Media. *J. Magn. Magn. Mater.* **2007**, *308*, 46.
7. Sun, Y.; Ding, X.; Zheng, Z.; Cheng, X.; Hua, X.; Peng, Y. Magnetic Separation of Polymer Hybrid Iron Oxide Nanoparticles Triggered by Temperature. *Chem. Commun.* **2006**, *26*, 2765–2767.
8. De Palma, R.; Peeters, S.; Van Bael, M. J.; Van den Rul, H.; Bonroy, K.; Laureyn, W.; Mullens, J.; Borghs, G.; Maes, G. Silane Ligand Exchange to Make Hydrophobic Superparamagnetic Nanoparticles Water-Dispersible. *Chem. Mater.* **2007**, *19*, 1821–1831.
9. Fan, Q.-L.; Neoh, K.-G.; Kang, E.-T.; Shuter, B.; Wang, S.-C. Solvent-Free Atom Transfer Radical Polymerization for the Preparation of Poly(ethyleneglycol) monomethacrylate)-Grafted Fe_3O_4 Nanoparticles: Synthesis, Characterization and Cellular Uptake. *Biomaterials* **2007**, *28*, 5426–5436.
10. Mornet, S.; Portier, J.; Duguet, E. A Method for Synthesis and Functionalization of Ultrasmall Superparamagnetic Covalent Carriers Based on Maghemite and Dextran. *J. Magn. Magn. Mater.* **2005**, *293*, 127–134.
11. Allen, T. M. The Use of Glycolipids and Hydrophilic Polymers in Avoiding Rapid Uptake of Liposomes by the Mononuclear Phagocyte System. *Adv. Drug Delivery Rev.* **1994**, *13*, 285–309.
12. Folkman, J. What is the Evidence That Tumors are Angiogenesis Dependent? *J. Natl. Cancer Inst.* **1990**, *82*, 4–7.
13. Brigger, I.; Dubernet, C.; Couvreur, P. Nanoparticles in Cancer Therapy and Diagnosis. *Adv. Drug Delivery Rev.* **2002**, *54*, 631–651.
14. Miller, J. C.; Pien, H. H.; Sahani, D.; Sorensen, G. A.; Thrall, J. H. Imaging Angiogenesis: Applications and Potential for Drug Development. *J. Natl. Cancer Inst.* **2005**, *97*, 172–187.
15. Iyer, A. K.; Khaled, G.; Fang, J.; Maeda, H. Exploiting the Enhanced Permeability and Retention Effect for Tumor Targeting. *Drug Discovery Today* **2006**, *11*, 812–818.
16. Papahadjopoulos, D.; Allen, T. M.; Gabizon, A.; Mayhew, E.; Matthay, K.; Huang, S. K. Sterically Stabilized Liposomes: Improvements in Pharmacokinetics and Antitumor Therapeutic Efficacy. *Proc. Natl. Acad. Sci. U.S.A.* **1991**, *88*, 11460–11464.
17. Zhang, Y.; Kohler, N.; Zhang, M. Surface Modification of Superparamagnetic Magnetite Nanoparticles and Their Intracellular Uptake. *Biomaterials* **2002**, *23*, 1553–1561.
18. Quinton, J.; Thomsen, L.; Dastoor, P. Adsorption of Organosilanes on Iron and Aluminium Oxide Surfaces. *Surf. Interface Anal.* **1997**, *25*, 931–936.
19. Mosmann, T. Rapid Colorimetric Assay for Cellular Growth and Survival: Application to Proliferation and Cytotoxicity Assays. *J. Immunol. Methods* **1983**, *65*, 55–63.
20. Howard, K. A.; Dash, P. R.; Read, M. L.; Ward, K.; Tomkins, L. M.; Nazarova, O.; Ulbrich, K.; Seymour, L. W. Influence of Hydrophilicity of Cationic Polymers on the Biophysical Properties of Polyelectrolyte Complexes Formed by Self-Assembly with DNA. *Biochim. Biophys. Acta* **2000**, *1475*, 245–255.
21. Raynal, I.; Prigent, P.; Peyramaure, S.; Najid, A.; Rebuzzi, C. Macrophage Endocytosis of Superparamagnetic Iron Oxide Nanoparticles. *Invest. Radiol.* **2004**, *39*, 56–63.
22. Zimmer, J. P.; Kim, S.-W.; Ohnishi, S.; Tanaka, E.; Frangioni, J. V.; Bawendi, M. G. Size Series of Small Indium Arsenide-Zinc Selenide Core−Shell Nanocrystals and Their Application to *In Vivo* Imaging. *J. Am. Chem. Soc.* **2006**, *128*, 2526–2527.
23. Corot, C.; Petry, K. G.; Trivedi, R.; Saleh, A.; Jonkmanns, C.; Le Bas, J. F.; Blezer, E.; Rausch, M.; Brochet, B.; Foster-Gareau, P.; Balériaux, D. Macrophage Imaging in Central Nervous System and in Carotid Atherosclerotic Plaque Using Ultrasmall Superparamagnetic Iron Oxide in Magnetic Resonance Imaging. *Invest. Radiol.* **2004**, *39*, 619–625.